







Complexity Reduction for Hybrid TOA/AOA Localization in UAV-Assisted WSNs

Le Chung Tran¹ , Anh Tuyen Le² , Xiaojing Huang² , Eryk Dutkiewicz² , Duy Ngo³ ,
and Attaphongse Taparugssanagorn⁴ 

¹School of Electrical, Computer, Telecommunications Engineering, University of Wollongong, Wollongong, NSW 2522, Australia

²School of Big Data, Engineering, University of Technology Sydney, Sydney, NSW 2007, Australia

³School of Engineering, University of Newcastle, Callaghan, NSW 2308, Australia

⁴School of Telecommunications, Information, Communications Technologies, Asian Institute of Technology, Pathum Thani 12120, Thailand

Manuscript received 27 August 2023; accepted 26 September 2023. Date of publication 9 October 2023; date of current version 17 October 2023.

Abstract—Unmanned aerial vehicles (UAVs)-assisted wireless sensor networks (WSNs) have tremendous potential applications due to their flexibility and rapid deployment. Hybrid time-of-arrival (TOA) and angle-of-arrival (AOA) localization techniques are commonly used due to their high accuracy. The conventional TOA/AOA localization algorithms require both zenith and azimuth angle estimations at each agent. Since a zenith-and-azimuth AOA estimation requires an L-shape antenna array and complicated 2-D signal processing, conventional TOA/AOA algorithms lead to both hardware and computational complexity and high power consumption at each agent. This letter proposes a hybrid TOA/AOA localization algorithm, named T1A_a, to reduce the agents' complexity. T1A_a only combines TOA-ranging with the azimuth angle estimation. Thereby, agents only require a 1-D antenna array, less complicated signal processing, and thus, lower power consumption. Such improvements are important for power-limited WSNs and Internet-of-Things (IoT) systems. Simulations are conducted to prove that the proposed T1A_a technique can achieve similar performance as conventional TOA/AOA methods, while significantly simplifying agents' complexity.

Index Terms—Sensor signal processing, angle-of-arrival (AOA), non-GPS localization, time-of-arrival (TOA), unmanned aerial vehicle (UAV), wireless sensor network (WSN).

I. INTRODUCTION

Hybrid time-of-arrival (TOA) and angle-of-arrival (AOA) localization is commonly used in wireless sensor networks (WSNs) due to its high accuracy. Conventional hybrid TOA/AOA algorithms require both azimuth and zenith angle estimations at each agent, especially when the agents move in a 3-D space [4]. It is shown in [5] and [6] that shadowing will greatly reduce TOA and AOA estimation accuracy. Therefore, using unmanned aerial vehicles (UAVs) as anchors can alleviate the problem of shadowing since there might be less obstruction and the line-of-sight path might be more likely to exist between the elevated drone and the agents [2]. To measure both azimuth and zenith angles, the beam of the antenna arrays at the agents must be steered in both horizontal and vertical planes, leading to heavily rotatable mechanical structures such as parabolic antennas, conical antennas, multiple log-periodic antennas [8], or complicated signal processing using L-shaped antennas [3].

To reduce the complexity and prolong the agents' battery working time, in [3], the authors propose a TOA/AOA localization algorithm, referred to as zenith TOA/1AOA (cf., Section II-B2 for more detail), where only TOA and zenith AOA information is used, rather than all TOA, namely azimuth and zenith AOA information, which is referred to as TOA/2AOA algorithm (see Section II-B1). This zenith TOA/1AOA algorithm has been shown to provide equivalent or even better accuracy than the conventional method when sufficient signal bandwidth or a sufficient number of UAVs is used. However, such zenith TOA/1AOA algorithm is relatively inferior compared to the conventional TOA/2AOA algorithm, at a low signal-to-noise ratio

range or when the signal bandwidth is limited. This Achilles heel presents even when agents move in a certain horizontal plane, such as the ground. There exist numerous practical applications, such as Internet-of-Things (IoT) for smart agriculture and localization for ground military operations, where the agents travel on a horizontal plane [6]. An important observation that could help overcome the drawback of the zenith TOA/1AOA algorithm is that, when agents move on the ground, the altitude of the agent is no longer an important factor. Thus, the measurement of azimuth angles is more important while the zenith AOA measurement is no longer needed.

In this letter, we propose a novel hybrid TOA/AOA localization algorithm, namely, the azimuth TOA/1AOA algorithm, where only azimuth AOA information is used to combine with TOA information for locating the agents. Simulations show that the proposed algorithm not only outperforms the zenith TOA/1AOA algorithm and approaches the performance of TOA/2AOA in many cases, but also has less computational complexity. Cramer-Rao lower bounds (CRLBs) are derived to provide benchmarks for these methods. In addition, the impacts of other parameters of the WSN, such as signal bandwidth, transmit power, UAVs' altitude, and the number of anchors, are evaluated, providing a useful tool for optimizing the complexity and positioning accuracy.

The contribution of this letter is the proposal of a novel azimuth TOA/1AOA localization method that not only provides good accuracy, but also requires simpler hardware and has less computational complexity than the two aforementioned counterparts.

II. HYBRID TOA/AOA LOCALIZATION

A. System Model

A WSN is deployed as in Fig. 1 including K UAV anchors with known locations at $\mathbf{a}_k = [x_k, y_k, z_k]^T$, $k = 1, \dots, K$, and M unknown

Corresponding author: Le Chung Tran (e-mail: lctran@uow.edu.au).

Associate Editor: F. Costa.

Digital Object Identifier 10.1109/LENS.2023.3322968

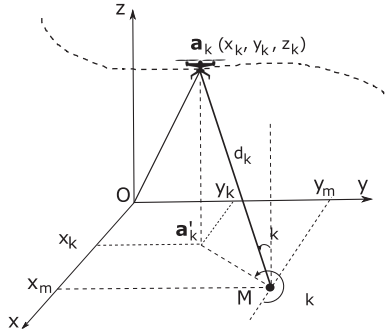


Fig. 1. Localization model in WSN with assisted UAVs.

agents denoted as $\mathbf{z}_m = [x_m, y_m, z_m]^T$, $m = 1, \dots, M$. It should be noted that the K UAV anchors here could be understood as either K different UAVs at known locations or K different way points of one UAV along its flight trajectory. For brevity, in this letter, the term K anchors might imply either case.

Assuming that all anchors and agents are in the communication ranges so that agents can perform TOA and AOA estimations from the beacons of all anchors. From TOA information, the estimated distance to the k th anchor is expressed as $\hat{d}_k = d_k + n_k$, for $k = 1, \dots, K$, where $d_k = \sqrt{(x_m - x_k)^2 + (y_m - y_k)^2 + (z_m - z_k)^2}$ is the real distance from the agent to the k th anchor, and n_k is the estimation error, which is assumed to be an independently and identically distributed (i.i.d.) Gaussian random variable with variance σ_d^2 , i.e., $n_k \sim \mathcal{N}(0, \sigma_d^2)$. Assuming the agent is equipped with a uniformly linear array (ULA), with N antenna elements separated by $\lambda/2$ from each other, where λ is the wavelength. The ULA is placed in parallel with the y -axis of the Cartesian coordinate system, thus its broadside is along the x -axis. From AOA estimation, azimuth and zenith angles, denoted as $\hat{\varphi}_k$ and $\hat{\theta}_k$, respectively, can be obtained as

$$\hat{\varphi}_k = \varphi_k + m_k; \quad \hat{\theta}_k = \theta_k + v_k \quad (1)$$

where φ_k and θ_k are the true azimuth and zenith angles, respectively, which are calculated by

$$\varphi_k = \begin{cases} \arctan\left(\frac{y_k - y_m}{x_k - x_m}\right), & x_k \leq x_m, y_k \leq y_m \\ \arctan\left(\frac{y_k - y_m}{x_k - x_m}\right) + \pi, & x_k > x_m \\ \arctan\left(\frac{y_k - y_m}{x_k - x_m}\right) + 2\pi, & x_k \leq x_m, y_k > y_m \end{cases} \quad (2)$$

and $\theta_k = \arccos\left(\frac{z_k - z_m}{d_k}\right)$; and m_k and v_k are the azimuth and zenith angle estimation errors, respectively. m_k and v_k are also modeled as i.i.d. zero-mean Gaussian random variables with variances $\sigma_{\varphi_k}^2$ and $\sigma_{\theta_k}^2$, respectively, i.e., $m_k \sim \mathcal{N}(0, \sigma_{\varphi_k}^2)$, $v_k \sim \mathcal{N}(0, \sigma_{\theta_k}^2)$.

B. Conventional TOA/2AOA and Zenith TOA/1AOA Localization

1) *Conventional TOA/2AOA Localization*: Conventionally, hybrid TOA and AOA localization uses the estimated range from TOA measurement combined with zenith and elevation angles to calculate the agent's position. From Fig. 1, the coordinates of the m th agent can be found by solving the following system of linear equations [9]:

$$\begin{aligned} x_m &= x_k + \hat{d}_k \sin \hat{\varphi}_k \cos \hat{\theta}_k \\ y_m &= y_k + \hat{d}_k \sin \hat{\varphi}_k \sin \hat{\theta}_k \\ z_m &= z_k - \hat{d}_k \cos \hat{\theta}_k, \quad \text{for } k = 1, \dots, K. \end{aligned} \quad (3)$$

In the matrix form, (3) can be expressed as

$$\mathbf{H}_I \mathbf{z}_m = \mathbf{b}_I \quad (4)$$

where $\mathbf{H}_I = \mathbf{I}_3 \otimes \mathbf{1}_K$ where \mathbf{I}_3 is the 3×3 identity matrix, \otimes denotes Kronecker product, $\mathbf{1}_K$ is a column vector of all ones, and $\mathbf{b}_I = [x_1 + \hat{d}_1 \sin \hat{\varphi}_1 \cos \hat{\theta}_1, \dots, x_K + \hat{d}_K \sin \hat{\varphi}_K \cos \hat{\theta}_K, y_1 + \hat{d}_1 \sin \hat{\varphi}_1 \sin \hat{\theta}_1, \dots, y_K + \hat{d}_K \sin \hat{\varphi}_K \sin \hat{\theta}_K, z_1 - \hat{d}_1 \cos \hat{\theta}_1, \dots, z_K - \hat{d}_K \cos \hat{\theta}_K]^T$. Equation (4) can be solved by a WLS solution [7] as $\hat{\mathbf{z}}_m = (\mathbf{H}_I^T \mathbf{W} \mathbf{H}_I)^{-1} \mathbf{H}_I^T \mathbf{W} \mathbf{b}_I$ where $\mathbf{W} = \text{diag}\{\sqrt{w_1}, \dots, \sqrt{w_K}\}$, with $w_k = 1 - \frac{\hat{d}_k}{\sum_{k=1}^K \hat{d}_k}$ as a weighting matrix to apply a higher weight on the shorter links, which gives more accurate estimation results as proved in [7]. This solution is denoted as T2A hereafter.

2) *Zenith TOA/1AOA Localization*: To reduce both hardware and computational complexities of each agent's terminal, in [3], TOA estimation is only combined with the zenith angle so that a single-dimensional antenna array is needed. As shown in [3], the WLS solution for this case is obtained as

$$\hat{\mathbf{z}}_m = (\mathbf{H}_{II}^T \mathbf{W}_{II} \mathbf{H}_{II})^{-1} \mathbf{H}_{II}^T \mathbf{W}_{II} \mathbf{b}_{II} \quad (5)$$

where $\mathbf{H}_{II} = 2 \begin{bmatrix} x_1 - x_r & y_1 - y_r \\ \vdots & \vdots \\ x_K - x_r & y_K - y_r \end{bmatrix}$, $\mathbf{H}_{II} \in \mathbb{R}^{(K-1) \times 3}$, $\mathbf{b}_{II} = [\hat{d}_r^2 \sin^2 \hat{\theta}_r - \hat{d}_1^2 \sin^2 \hat{\theta}_1 - r_r + r_1, \dots, \hat{d}_r^2 \sin^2 \hat{\theta}_r - \hat{d}_K^2 \sin^2 \hat{\theta}_K - r_r + r_K]^T$, $r_k = x_k^2 + y_k^2$, $k = 1, \dots, K$, and $k \neq r$; and \mathbf{W}_{II} is a $(K-1) \times (K-1)$ diagonal matrix whose the diagonal element is $w_{II}(k, k) = 1 - \frac{|\hat{d}_k \sin \hat{\theta}_k|}{\sum_k |\hat{d}_k \sin \hat{\theta}_k|}$, $k = 1, \dots, K$ and $k \neq r$. The solution in (5) using TOA and AOA zenith angle is denoted as T1A_z.

It is noted that, for the T1A_z algorithm, we have (cf., [3, eq.(10)])

$$(x_m - x_k)^2 + (y_m - y_k)^2 = \hat{d}_k^2 \sin^2 \hat{\theta}_k, \quad k = 1, \dots, K. \quad (6)$$

C. Proposed Azimuth TOA/1AOA Localization

In many applications, when agents move on a flat surface or the agents' altitude is unimportant, we propose a new method to combine TOA and azimuth AOA estimations as follows. Assuming agents are on the ground, i.e., $z_m = 0$, $m = 1, \dots, M$, the location of the m th agent is determined by

$$x_m = x_k + \sqrt{\hat{d}_k^2 - z_k^2} \cos(\hat{\varphi}_k), \quad y_m = y_k + \sqrt{\hat{d}_k^2 - z_k^2} \sin(\hat{\varphi}_k) \quad (7)$$

or in the matrix form

$$\mathbf{H} \begin{bmatrix} x_m \\ y_m \end{bmatrix} = \mathbf{b} \quad (8)$$

where $\mathbf{H} = \mathbf{1}_K \otimes \mathbf{I}_2$ and $\mathbf{b} = [x_1 + \sqrt{\hat{d}_1^2 - z_1^2} \cos \hat{\varphi}_1, y_1 + \sqrt{\hat{d}_1^2 - z_1^2} \sin \hat{\varphi}_1, \dots, x_K + \sqrt{\hat{d}_K^2 - z_K^2} \cos \hat{\varphi}_K, y_K + \sqrt{\hat{d}_K^2 - z_K^2} \sin \hat{\varphi}_K]^T$. Using the WLS method to solve (8), we get the position of the agent as

$$\mathbf{z}_m = (\mathbf{H}^T \mathbf{W} \mathbf{H})^{-1} \mathbf{H}^T \mathbf{W} \mathbf{b}. \quad (9)$$

The solution in (9) is referred to as T1A_a.

From (7), it is clear that

$$(x_m - x_k)^2 + (y_m - y_k)^2 = \hat{d}_k^2 - z_k^2, \quad \text{for } k = 1, \dots, K. \quad (10)$$

Unlike (6) where the accuracy of the agent's estimated coordinates is affected by both distance and zenith angle measurement errors, (10) shows that the accuracy in the azimuth TOA/1AOA algorithm does not depend on the zenith angle measurement errors. As a result, the accuracy of the proposed azimuth TOA/1AOA algorithm will be higher

than that of the zenith TOA/1AOA algorithm. This observation will be confirmed later in our simulations.

III. CRAMER-RAO LOWER BOUND (CRLB)

The CRLB is a common benchmark to compare different localization algorithms. CRLBs for T2A, zenith T1A_z, and the proposed azimuth T1A_a algorithms are derived as follows.

A. Hybrid TOA/2AOA for 3-D Agents

Denoting TOA and AOA estimators in the hybrid T2A as $\hat{\mathbf{a}}_{\text{T2A}} = [\hat{d}_1, \dots, \hat{d}_K, \hat{\varphi}_1, \dots, \hat{\varphi}_K, \hat{\theta}_1, \dots, \hat{\theta}_K]^T \in \mathbb{R}^{3K \times 1}$. The vector $\hat{\mathbf{a}}_{\text{T2A}}$ carries the information of the unknown parameters in $\hat{\mathbf{a}}_{\text{T2A}}$.

According to [1], the TOA estimation error is determined by the received signal-to-noise ratio (SNR), number of antenna elements N , and mean effective bandwidth B of the transmitted signal, i.e.,

$$\sigma_{d_k} \geq \frac{c}{\sqrt{2N\text{SNR}_k B}} \quad (11)$$

where c is the speed of light, while the lower bounds of σ_{φ_k} and σ_{θ_k} are

$$\sigma_{\varphi_k} \geq \sqrt{\frac{3}{(N-1)N(2N-1)\pi^2\text{SNR}_k \sin^2 \varphi_k}} \quad (12)$$

$$\sigma_{\theta_k} \geq \sqrt{\frac{3}{(N-1)N(2N-1)\pi^2\text{SNR}_k \sin^2 \theta_k}}. \quad (13)$$

The CRLB of an estimator is derived from a Fisher information matrix (FIM), which can be calculated from the log-likelihood function of the estimated vector. The likelihood function of $\hat{\mathbf{a}}_{\text{T2A}}$, conditioned on \mathbf{z} , denoted as $f(\hat{\mathbf{a}}_{\text{T2A}}; \mathbf{z})$, is

$$f(\hat{\mathbf{a}}_{\text{T2A}}; \mathbf{z}) = \prod_{k=1}^K \frac{1}{2\sqrt{2}\pi^3 \sigma_{d_k} \sigma_{\varphi_k} \sigma_{\theta_k}} e^{-\left[\frac{(d_k - \hat{d}_k)^2}{2\sigma_{d_k}^2} + \frac{(\varphi_k - \hat{\varphi}_k)^2}{2\sigma_{\varphi_k}^2} + \frac{(\theta_k - \hat{\theta}_k)^2}{2\sigma_{\theta_k}^2} \right]}. \quad (14)$$

Assuming that the estimations of d_k , φ_k , and θ_k are unbiased, i.e., $E\{\hat{d}_k\} = d_k$, $E\{\hat{\varphi}_k\} = \varphi_k$, and $E\{\hat{\theta}_k\} = \theta_k$, following the same steps shown in [10], the CRLB of the T2A estimator is $\text{CRLB}_{\text{T2A}} = \sqrt{\text{Tr}(\mathbf{F}_{\text{T2A}}^{-1})}$, where $\mathbf{F}_{\text{T2A}} = E\{(\mathbf{D}_{\text{T2A}})^T \mathbf{R}_{\text{T2A}} \mathbf{D}_{\text{T2A}}\}$ is the FIM of T2A,

$$\mathbf{R}_{\text{T2A}} = \text{diag}\left(\sigma_{d_1}^{-2}, \dots, \sigma_{d_K}^{-2}, \sigma_{\varphi_1}^{-2}, \dots, \sigma_{\varphi_K}^{-2}, \sigma_{\theta_1}^{-2}, \dots, \sigma_{\theta_K}^{-2}\right),$$

$$\mathbf{D}_{\text{T2A}} = \begin{bmatrix} \frac{x_m - x_1}{d_1} & \frac{y_m - y_1}{d_1} & \frac{z_m - z_1}{d_1} \\ \vdots & \vdots & \vdots \\ \frac{x_m - x_K}{d_K} & \frac{y_m - y_K}{d_K} & \frac{z_m - z_K}{d_K} \\ -\frac{(y_m - y_1)}{s_1^2} & \frac{(x_m - x_1)}{s_1^2} & 0 \\ \vdots & \vdots & \vdots \\ -\frac{(y_m - y_K)}{s_K^2} & \frac{(x_m - x_K)}{s_K^2} & 0 \\ \frac{(x_m - x_1)(z_m - z_1)}{d_1^2 s_1} & \frac{(y_m - y_1)(z_m - z_1)}{d_1^2 s_1} & \frac{-s_1}{d_1} \\ \vdots & \vdots & \vdots \\ \frac{(x_m - x_K)(z_m - z_K)}{d_K^2 s_K} & \frac{(y_m - y_K)(z_m - z_K)}{d_K^2 s_K} & \frac{-s_K}{d_K} \end{bmatrix} \quad (15)$$

and $s_k = \sqrt{(x_m - x_k)^2 + (y_m - y_k)^2}$, for $k = 1, \dots, K$.

B. Zenith TOA/1AOA for Ground Agents

As this letter focuses on the applications where agents move on a certain horizontal plane where their z-coordinates are constant, the measurement of the parameter z_m is no longer needed. As a result, we consider the vector of unknown parameter $\mathbf{z}_m = [x_m, y_m]^T$. The FIM

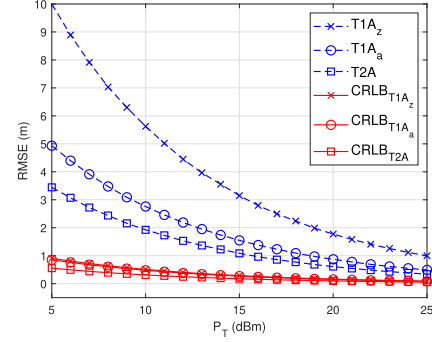


Fig. 2. RMSE (m) versus transmit power (dBm) with the UAV altitude of 300 m and bandwidth of 500 kHz.

of T1A_z can be written as $\mathbf{F}_{\text{T1A}_z} = E\{(\mathbf{D}_{\text{T1A}_z})^T \mathbf{R}_{\text{T1A}_z} \mathbf{D}_{\text{T1A}_z}\}$. $\mathbf{D}_{\text{T1A}_z}$ is the $2K \times 2$ -sized submatrix of \mathbf{D}_{T2A} , formed by taking elements in the first and second columns of the first K rows and the last K rows of \mathbf{D}_{T2A} . Meanwhile, $\mathbf{R}_{\text{T1A}_z} = \text{diag}(\sigma_{d_1}^{-2}, \dots, \sigma_{d_K}^{-2}, \sigma_{\theta_1}^{-2}, \dots, \sigma_{\theta_K}^{-2})$. The CRLB of the zenith T1A is $\text{CRLB}_{\text{T1A}_z} = \sqrt{\text{Tr}(\mathbf{F}_{\text{T1A}_z}^{-1})}$.

C. Azimuth TOA/1AOA for Ground Agents

The observation vector of azimuth T1A is written as $\hat{\mathbf{a}}_{\text{T1A}_a} = [\hat{d}_1, \dots, \hat{d}_K, \hat{\varphi}_1, \dots, \hat{\varphi}_K]^T \in \mathbb{R}^{2K}$. Following the same steps as aforementioned, the FIM of T1A_a is calculated as $\mathbf{F}_{\text{T1A}_a} = E\{(\mathbf{D}_{\text{T1A}_a})^T \mathbf{R}_{\text{T1A}_a} \mathbf{D}_{\text{T1A}_a}\}$, where the $2K \times 2$ -sized $\mathbf{D}_{\text{T1A}_a}$ matrix is obtained by taking elements in the first and second columns of the first $2K$ rows of \mathbf{D}_{T2A} , and $\mathbf{R}_{\text{T1A}_a} = \text{diag}(\sigma_{d_1}^{-2}, \dots, \sigma_{d_K}^{-2}, \sigma_{\varphi_1}^{-2}, \dots, \sigma_{\varphi_K}^{-2})$.

The CRLB of the azimuth T1A is $\text{CRLB}_{\text{T1A}_a} = \sqrt{\text{Tr}(\mathbf{F}_{\text{T1A}_a}^{-1})}$.

IV. SIMULATION RESULTS AND ANALYSES

Simulations are conducted in MATLAB to evaluate the performance of the proposed azimuth TOA/1AOA and compare it to that of the conventional TOA/2AOA and zenith TOA/1AOA. For brevity, in the following figures, we denote the three algorithms as T1A_a, T2A, and T1A_z, respectively. Four UAVs are randomly deployed at the altitude $h = 300$ m transmitting beacons to ten agents traveling in an area of $1000 \text{ m} \times 1000 \text{ m}$. Path loss model follows the one in [3]. The noise spectral density is -174 dBm/Hz. The beacons with bandwidth B are transmitted over 2-GHz carrier frequency and the power P_T dBm. Each agent is equipped with an antenna array of ten elements, spacing at half the wavelength for performing TOA and AOA estimations. Using (11) and (12), the standard deviations of estimation noises σ_{d_k} , σ_{φ_k} , and σ_{θ_k} can be obtained. Since the agents are assumed to travel in a 2-D plane, the root mean square error (RMSE) to compare different localization algorithms is calculated as

$$\text{RMSE} = \sqrt{E\left\{\frac{1}{M} \sum_{m=1}^M [(x_m - \hat{x}_m)^2 + (y_m - \hat{y}_m)^2]\right\}} \quad (16)$$

where $E\{\cdot\}$ stands for expectation over Monte Carlo simulations.

Fig. 2 presents the RMSE of the proposed T1A_a algorithm compared to those of T1A_z and T2A and the CRLBs of these methods accordingly. It is obvious that the proposed T1A_a performs much better than T1A_z and approaches T2A's performance, especially when the transmit power is higher than 20 dBm. In the low transmission power condition, T1A_a achieves a significant improvement compared to T1A_z, with the RMSE of the former being only half of that of the latter when $P_T = 5$ dBm.

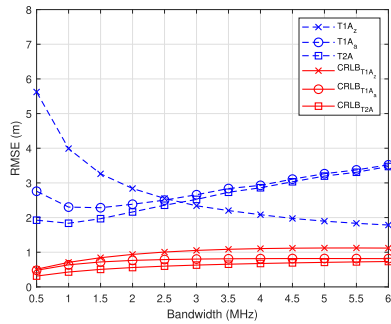


Fig. 3. RMSE (m) versus signal bandwidth (MHz) with the UAV altitude of 300 m and transmit power of 10 dBm.

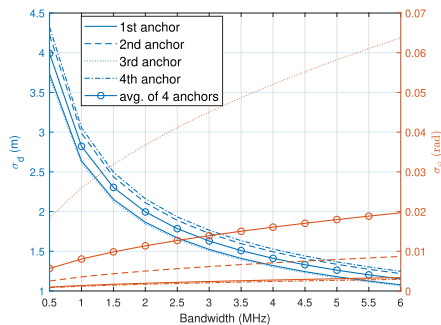


Fig. 4. Dependence of σ_d (m) and σ_ϕ (rad) on bandwidth with the UAV altitude of 300 m.

We then evaluate the mentioned methods under different transmit signal bandwidths. Fig. 3 shows the proposed $T1A_a$ algorithm's performance compared with that of $T1A_z$ and T2A counterparts over a range of signal bandwidth from 500 kHz to 6 MHz with the transmit power $P_T = 10$ dBm. The figure confirms that the proposed $T1A_a$ approaches the T2A algorithm and outperforms $T1A_z$ algorithm at a low-to-medium signal bandwidth.

It can also be seen from Fig. 3 that, with the increase of the signal bandwidth, the accuracy of $T1A_a$ and T2A first tends to improve and then reduce, while that of $T1A_z$ improves. To explain this phenomenon, the dependence of σ_{d_k} and σ_{ϕ_k} on the signal bandwidth are plotted in Fig. 4. The transmitted power $P_T = 10$ dBm is considered in this simulation. Clearly, when the bandwidth increases, σ_{d_k} reduces exponentially fast, while σ_{ϕ_k} increases exponentially. This is because σ_{d_k} is inversely proportional to both signal bandwidth and SNR [cf., (11)]. Meanwhile, σ_{ϕ_k} only depends on SNR [cf., (12)], which reduces due to increasing noise over a wider bandwidth. Therefore, when the bandwidth increases, σ_{ϕ_k} becomes higher, leading to less accurate $T1A_a$ and T2A. This confirms that the signal bandwidth of the WSN with the proposed $T1A_a$ can be reduced while maintaining the accuracy performance at an acceptable level.

The impacts of the number of anchors and their height on the performance of the proposed algorithm are examined. Fig. 5 shows the performance of the three algorithms when 4–10 anchors are used under two cases of UAV's altitudes of 300 and 500 m, respectively. We can see that the anchors' altitude has a significant impact on the performance of both $T1A_a$ and $T1A_z$ algorithms, while it is much less significant in the case of T2A. In addition, when UAVs are flying at a certain altitude above the ground, having more UAVs improves the performance of all algorithms. However, while the number of anchors has a significant impact on the accuracy of $T1A_z$, it has less significance for the cases of $T1A_a$ and T2A. Hence, with the proposed $T1A_a$, the number of anchors can be reduced compared to $T1A_z$. This will translate into less complex signal processing, lower localization latency, and more power saving.

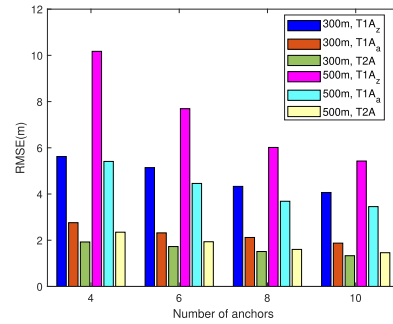


Fig. 5. Localization accuracy versus number of anchors with the UAV altitudes of 300 and 500 m, transmit power of 10 dBm, and bandwidth of 500 kHz.

TABLE 1. Comparison of Computational Complexity

	$T1A_a$	$T1A_z$	T2A
Average elapsed time (s)	3.6654e-05	4.4095e-05	5.3345e-05

Finally, Table 1 compares the average elapsed time (in seconds) of the three algorithms. Clearly, the computational complexity of the proposed azimuth TOA/IAOA is the best among the three algorithms.

V. CONCLUSION

This letter evaluates different approaches using hybrid TOA/AOA localization algorithms. A novel way of combining TOA ranging information and azimuth AOA estimation has been proposed. We prove that when the altitudes of agents remain unchanged or on the ground plane, combining TOA and azimuth AOA estimations can achieve almost the same level of accuracy as conventional hybrid schemes where TOA is combined with both azimuth and zenith AOA estimations. The proposed method also outperforms our previous findings which use TOA and zenith AOA estimations, especially when the transmit power or the signal bandwidth is limited. The proposed method, therefore, significantly reduces the complexity of agents and power consumption of WSNs with assisted UAVs.

REFERENCES

- [1] Y. Fu and Z. Tian, "Cramer-Rao bounds for hybrid TOA/DOA-based location estimation in sensor networks," *IEEE Signal Process. Lett.*, vol. 16, no. 8, pp. 655–658, Aug. 2009.
- [2] A. F. G. Gonçalves Ferreira, D. M. A. Fernandes, A. P. Catarino, and J. L. Monteiro, "Localization and positioning systems for emergency responders: A survey," *IEEE Commun. Surv. Tuts.*, vol. 19, no. 4, pp. 2836–2870, Fourth Quarter 2017.
- [3] A. T. Le et al., "Hybrid TOA/AOA localization with 1 angle estimation in UAV-assisted WSN," in *Proc. IEEE 14th Int. Conf. Signal Process. Commun. Syst.*, 2020, pp. 1–6.
- [4] Y. Liu, Y. Wang, Y. Shen, and X. Shi, "Hybrid TOA-AOA WLS estimator for aircraft network decentralized cooperative localization," *IEEE Trans. Veh. Technol.*, vol. 19, no. 4, pp. 2836–2870, Jul. 2023.
- [5] N. M. Nguyen et al., "Performance evaluation of non-GPS based localization techniques under shadowing effects," *Sensors*, vol. 19, no. 11, pp. 2633–1–2633–21, 2019.
- [6] A. Pandey, P. Tiwary, S. Kumar, and S. K. Das, "FadeLoc: Smart device localization for generalized $\kappa-\mu$ faded IoT environment," *IEEE Trans. Signal Process.*, vol. 70, pp. 3206–3220, 2022.
- [7] S. Tomic, M. Beko, R. Dinis, and P. Montezuma, "A closed-form solution for RSS/AoA target localization by spherical coordinates conversion," *IEEE Wireless Commun. Lett.*, vol. 5, no. 6, pp. 680–683, Dec. 2016.
- [8] J. L. Volakis, *Antenna Engineering Handbook*. New York, NY, USA: McGraw-Hill Education, 2007.
- [9] K. Yu, "3-D localization error analysis in wireless networks," *IEEE Trans. Wireless Commun.*, vol. 6, no. 10, pp. 3472–3481, Oct. 2007.
- [10] K. Yu, I. Sharp, and Y. J. Guo, *Ground-Based Wireless Positioning*. Chichester, U.K.: Wiley, 2009.